



Published in final edited form as:

Angew Chem Int Ed Engl. 2021 September 01; 60(36): 19660–19664. doi:10.1002/anie.202105679.

Enantioselective Addition of Pyrazoles to Dienes

Alexander Y. Jiu^b, Hannah S. Slocumb^b, Charles S. Yeung^c, Xiao-Hui Yang^a, Vy M. Dong^b

^[a]Prof. Dr. X.-H. Yang, Advanced Research Institute of Multidisciplinary Science, and School of Chemistry and Chemical Engineering, Beijing Institute of Technology, Beijing 100081, China

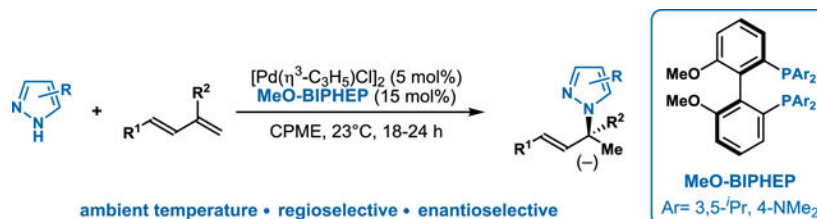
^[b]A. Y. Jiu, H. S. Slocumb, Prof. Dr. V. M. Dong, Department of Chemistry, University of California, Irvine, Irvine, CA 92697 (USA)

^[c]Dr. C. S. Yeung, Discovery Chemistry, Merck & Co., Inc., Boston, MA 02115 (USA), United States

Abstract

We report the first enantioselective addition of pyrazoles to 1,3-dienes. Secondary and tertiary allylic pyrazoles can be generated with excellent regioselectivity. Mechanistic studies support a pathway distinct from previous hydroaminations: a Pd(0)-catalyzed ligand-to-ligand hydrogen transfer (LLHT). This hydroamination tolerates a range of functional groups and advances the hydrofunctionalization of dienes.

Graphical Abstract



Keywords

pyrazole; 1,3-diene; hydroamination; Pd-catalysis; enantioselectivity

Nitrogen-containing heterocycles, such as pyrazoles, represent valuable scaffolds for drug discovery and thus remain an inspiration for synthetic methods (Figure 1A).¹ The direct addition of a pyrazole to a double bond represents an attractive and atom-economical approach for forging C-N bonds. With regards to the coupling partner, conjugated dienes are ideal building blocks,² with many being raw materials for various industrial applications, including polymerizations.^{3,4} Within the asymmetric hydroamination of dienes, there exists methods using anilines (Hartwig),⁵ secondary amines (our lab and Malcolmson),^{6,7} and primary amines (Mazet).⁸ In comparison to previously studied amines (with nucleophilicities $N = 13-18$ on Mayr scale⁹), pyrazoles present a challenge and

opportunity because of their lower nucleophilicity ($N = 9.6$). Given the two reactive nitrogen atoms: a pyrrolic and a pyridinic nitrogen, the coupling of pyrazoles with unsymmetrical dienes can provide 32 isomers (Figure 1B). With both Rh and Pd-catalysts, Breit achieved enantioselective hydroamination of allenes using pyrazoles (Figure 1C).¹⁰ Concurrent with our studies, Chen and coworkers were independently pursuing the Pd-catalyzed hydroamination of isoprene. With indazoles and select pyrazoles, they were able to generate either achiral or racemic products.¹¹ In this communication, we showcase the first asymmetric addition of pyrazoles to dienes. This mild hydroamination tolerates a variety of functional groups and occurs via a mechanism distinct to those previously proposed for diene hydroamination.

On the basis of our previous hydroaminations of dienes, we initiated investigations with Rh-catalysts.^{6,12} We chose pyrazole (**1a**) and 1-phenyl-butadiene (**2a**) as the model substrates and observed no desired reactivity (see SI). In contrast, under Pd-catalysis, the desired allylated pyrazole **3aa** was obtained when using a range of achiral bisphosphine ligands (see SI). In search of an asymmetric variant (**L1–L8**), we found that atropisomeric bisphosphine ligands gave the most promising results (Table 1). Thus, we focused on this ligand family to achieve enantioselective catalysis. The DTBM analogs **L5–L7** afford desired pyrazole **3aa** in 70–82% yield and good to excellent selectivity (>20:1 *rr*, 90:10–95:5 *er*). Substitution on the aryl groups most likely enhances reactivity by promoting ligand-substrate dispersion interactions in the transition state, a concept in accordance with literature observations by Buchwald and others.¹³ We observed similar ligand trends in Rh-catalyzed hydrofunctionalizations of alkynes.¹⁴ With further optimization¹⁵, we found commercially available MeO-BIPHEP ligand **L8** afforded **3aa** in 91% yield with >20:1 *rr* and 96:4 *er*.

With **L8** in hand, we examined the addition of various pyrazoles **1** to diene **2a** (Table 2). Generally, allylated pyrazoles **3ab–3aj** form with high enantioselectivity (88:12–97:3 *er*) and >20:1 *rr* in the coupling of diene **2a** with pyrazoles **1b–1j**. The electronic properties of the pyrazoles show negligible impact on enantioselectivity and regioselectivity. However, electron-withdrawing substituents show more sluggish reactivity and require extended reaction times (**3ad–3af, 3aj**) or higher temperature (**3ag, 3ah**) to obtain good yields (64–86%). Halogenated products (**3ad, 3ae**) are tolerated despite the potential for competing oxidative addition into the aryl halide bond; no side products from oxidative addition are observed. Electron-donating substituents allow for facile reactivity and shorter reaction times (**3ai**, 69%, 89:11 *er*). Other unsymmetrical pyrazoles provide moderate to excellent $N^1:N^2$ regioselectivity (**3ak–3am**, 11:1–20:1 *rr*). The $N^1:N^2$ regioselectivity favors allylation at the less sterically-congested nitrogen atom. Pyrazole tautomerization is known to occur in solution; for example, 5-Me pyrazole (**1k**) exists in a nearly 1:1 ratio of the 3- and 5-substituted pyrazoles on the basis of NMR spectroscopy.¹⁵ Despite the presence of tautomers, we observe high selectivity for formation of **3ak**, which indicates tautomerization occurs faster than C–N bond formation. Together, these results represent the first enantioselective hydroamination of 1,3-dienes with azoles.¹⁶

In addition to pyrazole substrates, several other azoles show promising reactivity under the standard conditions. The addition of 1H-1,2,3-triazole (**3an**) gives 70% yield and 91:9 *er*

with high regioselectivity (>20:1 *rr*, >20:1 *N*²:*N*¹).¹⁷ The coupling of 1H-benzotriazole, 1H-indazole, and 2-butyl-1H-imidazole with diene **2a** provides the corresponding allylated azoles (**3ao**, **3ap**, and **3aq**) with promising reactivity and chemoselectivity, however, further optimization is needed.¹⁸ In stark contrast, pyrrole showed no reactivity, a result that supports our hypothesis on the mechanism (*vide infra*).

Next, we studied the hydroamination of fourteen different 1,3-dienes **2** with pyrazole **1a** (Table 3). Varying substitution on the aryl dienes results in a range of chiral allylated pyrazoles **3ba–3ka** (31–95% yield, >20:1 *rr*, 89:11–96:4 *er*). Both electron-rich methoxy-substituted (**3ba**, **3fa**, and **3ha**) and electron-poor fluoro-substituted (**3ea**) 1,3-dienes react well. In contrast, chloro-substituted phenyl diene **2d** affords **3da** in only 31% yield due to competing oxidative addition into the C–Cl bond. Sterically encumbered *ortho*-substituted dienes undergo addition to **3ha** and **3ia** in 40% and 62% yield, respectively. The protocol transforms heterocyclic substituted dienes **2j** (*R*¹ = 2-furyl) and **2k** (*R*¹ = 2-thiophene) into **3ja** in 34% yield, 90:10 *er*, and >20:1 *rr*, and **3ka** in 95% yield, 93:7 *er*, and >20:1 *rr*. Hydroamination of alkyl substituted 1,3-diene **2l** yields the allylic pyrazole **3la** in 45% yield, 95:5 *er*, and 2:1 *rr*. Cyclic dienes such as 1,3-cyclohexadiene (**2m**) couple with pyrazole (**1a**) to generate **3ma** in 71% yield and >20:1 *rr*, albeit with a lower enantioselectivity of 81:19 *er*. Hydroamination of feedstocks, isoprene and myrcene, provide the tertiary allylic amines (**3na**, **3oa**) as single structural isomers.

Electronic circular dichroism (ECD) is a powerful technique to determine absolute configuration.¹⁹ By using this method, we elucidated the absolute stereochemistry of the chiral allylated azoles. Comparing theoretical calculations and experimental data, a qualitative match (i.e., similar shapes) enabled assignment of the absolute configuration.¹⁹ TDDFT calculations produced the ECD spectra of (*S*)-**3aa** and (*S*)-**3ab**. Qualitative comparison to the experimental results suggests that the major enantiomer bears the (*S*)-configuration as drawn (see SI).

Previous reports on the hydrofunctionalization of dienes, including Chen's hydroamination of isoprene, feature mechanisms that occur by Pd(II)–H catalysis.^{4,11} In these scenarios, alkene insertion into a Pd–H forges the new carbon-hydrogen bond and these transformations occur at elevated temperatures. On the basis of recent reports and our own observations, we propose that our ambient hydroamination occurs via the mechanism depicted in Figure 3. The palladium pre-catalyst interacts with a bisphosphine ligand to form active Pd(0) catalyst **I**. Both pyrazole **1** and 1,3-diene **2** bind to complex **I** to generate palladium intermediate **II**. Given Pd(II)'s preference to adopt a square planar geometry, we reason that diene coordinates to the Pd in an η² fashion.^{11,20,21} From here, we imagine that the hydrogen atom is transferred directly from pyrazole **1** to 1,3-diene **2** through ligand-to-ligand hydrogen transfer (LLHT). Ionization of intermediate **III** followed by outer-sphere nucleophilic attack with pyrazole anion on the C3 carbon affords the desired allylic pyrazole **3** and regenerates Pd(0) complex **I**.

In support of a Pd(0) pathway, Huang²² and Rutjes²³ computations have shown that the formation of the Pd(II)–H complex from [Pd(η³-C₃H₅)Cl]₂ is kinetically infeasible at temperatures up to 80°C. In line with this, we do not observe Pd–H when studying a mixture

of $[\text{Pd}(\eta^3\text{-C}_3\text{H}_5)\text{Cl}]_2$ with ligand in *d*₈-toluene. Additionally, alternative Pd(0) precursors, including Pd(PPh₃)₄ and Pd(P^tBu₃)₂, afford the allylic pyrazole albeit in lower yields and selectivity (see SI). In these cases, there is no acid additive, which makes Pd–H unlikely. By using Burés' variable time normalization analysis (VTNA) method,²⁴ we studied the kinetic profile and observed first order in catalyst and zero order in both the pyrazole (**1**) and diene (**2**). This rate law supports coordination of diene and pyrazole to Pd to generate intermediate **II** as the catalyst resting state.

In Zi's study on hydrosulfonylation of dienes, theoretical calculations show that diene migratory insertion into Pd(II)–H is energetically unfavorable compared to LLHT.²⁰ In analogy, we propose an LLHT that is the turnover-limiting step (Figure 3). Comparing the initial rates of deuterated pyrazole **d-1a** against 1H-pyrazole **1a** in parallel, we observe a KIE of 1.4 (Figure 4A) which is similar with previous LLHT examples.²⁵ When we subjected deuterium-labeled pyrazole **d-1a** to the standard conditions (Figure 4B), we see quantitative deuterium incorporation at the C4 position of **d-3aa**; the recovered diene shows no deuterium labelling. Together, these results suggest that hydrogen transfer is highly selective and irreversible. Of note, in Malcolmson's hydroamination, the analogous experiment demonstrated deuterium scrambling.⁷ Additionally, hydroamination of diene **1a** with pyrrole shows no reactivity. In comparison to pyrazole, the pyrrole lacks a second nitrogen atom. We reason the second nitrogen coordinates to Pd to provide the geometry needed for LLHT.

Next, we performed a crossover study by adding pyrazole **1b** to (*S*)-**3aa** in the presence of the Pd-catalyst (Figure 4C, entry 1). The crossover product (*S*)-**3ab** was generated where the major isomer possessed the same absolute configuration as the (*S*)-**3aa** starting material. A similar crossover experiment using a racemic mixture of **3aa** was performed (Figure 4C, entry 2). After 18 h, the crossover product (*S*)-**3ab** (60:40 *er*) is afforded along with an enantioenriched mixture of (*R*)-**3aa** (34:66 *er*). Enantioenrichment of the *R*-enantiomer suggests that (*S*)-**3aa** reacts faster, transforming into (*S*)-**3ab** in these crossover experiments. These experiments suggest that Pd insertion into the C–N bond can be reversible, especially under conditions where pyrazole is present in large excess (see SI). We found that the use of excess diene affords better results and reason that this stoichiometry prevents reversible product formation. Based on these experiments, we favor a mechanism that involves outer sphere nucleophilic attack of pyrazole to complex **III**. In line with Tsuji–Trost transformations, the ionization of allylic pyrazole (*S*)-**3** with Pd-catalyst would invert the configuration at the reactive center (Figure 4C). To afford the *S*-enantiomer of the crossover product, the nucleophile must attack through an S_N2-like mechanism on the face of the olefin opposite to Pd. Our proposed mechanism fits with the convention of classifying nucleophilic attack on $\eta^3\text{-Pd-}\pi\text{-allyl}$ intermediates. Pyrazole, which is considered a “soft” nucleophile ($\text{p}K_{\text{a}} \sim 19.8$), would be expected to proceed through this outer-sphere pathway.²⁶

In our and Malcolmson's independently reported Pd-catalyzed diene hydrofunctionalizations, a competition experiment was performed using a mixture of *E* and *Z* dienes. In their studies, both (*Z*)- and (*E*)-1-phenylbutadiene (**2a**) converged to the same major enantiomer.^{7,27} Moreover, deuterium scrambling into the diene was observed. These results supported a Pd–H mechanism where hydropalladation is reversible. In this

pyrazole study, however, we find when using a mixture of (*Z*)- and (*E*)-1-phenylbutadiene (**2a**) isomers, only the (*E*)-**2a** transforms to allylic pyrazole (**3aa**) (50% yield brsm), while the (*Z*)-**2a** is recovered (Figure 4D). These contrasting results point to a mechanism which differs from those previously invoked. Here, we reason that the (*Z*)-diene does not transform due to increased steric strain in the LLHT step.

Hydroamination represents an attractive way to transform dienes into nitrogen-containing building blocks. By using Pd-catalysis, we achieved the first enantioselective hydroamination of dienes with aromatic heterocycles. The allylation tolerates a broad range of substituted pyrazoles and dienes, and both secondary and tertiary allylated pyrazoles are obtained in good to excellent yields with high regio- and enantioselectivities. Insights from this study will guide the development of related couplings that feature heterocycles, which represent motifs pertinent in drug discovery.

Supplementary Material

Refer to Web version on PubMed Central for supplementary material.

Acknowledgements

Funding provided by UC Irvine, the National Institutes of Health (1R35GM127071) and the National Science Foundation (CHE-1465263). X.-H. Y. thanks the Beijing Institute of Technology Teli Young Fellow Project. We thank Solvias AG for donating commercial MeO-BIPHEP **L8**. We thank Lisa M. Nogle, David A. Smith, Adam Beard, Mirosława Darlak, and Mark Pietrafitta for reversed phase purifications (Merck & Co., Inc.). We thank Donovan Adressa for assistance with NMR structure elucidation (Merck & Co., Inc.). This work utilized the infrastructure for high-performance and high-throughput computing, research data storage and analysis, and scientific software tool integration built, operated, and updated by the Research Cyber infrastructure Center (RCIC) at the University of California, Irvine (UCI). The RCIC provides cluster-based systems, application software, and scalable storage to directly support the UCI research community. <https://rcic.uci.edu>.

References

- (1). Vitaku E, Smith DT, Njardson JT, J. Med. Chem. 2014, 57, 10257–10274. [PubMed: 25255204]
- (2). For selected reviews on 1,3-dienes as building blocks, see: (a)Reymond S, Cossy J, Chem. Rev. 2008, 108, 5359–5406; [PubMed: 18942879] (b)Zhu Y, Cornwall RG, Du H, Zhao B, Shi Y, Acc. Chem. Res. 2014, 47, 3665–3678; [PubMed: 25402963] (c)Chen J-R, Hu X-Q, Lu L-Q, Xiao W-J, Chem. Rev. 2015, 115, 5301–5365. [PubMed: 25992465]
- (3). For selected reviews on polymerization of 1,3-dienes, see: (a)Ricci G, Sommazzi A, Masi F, Ricci M, Boglia A, Leone G, Coord. Chem. Rev. 2010, 254, 661;(b)Valente A, Mortreux A, Visseaux M, Zinck P, Chem. Rev. 2013, 113, 3836–3857; [PubMed: 23391234] (c)Takeuchi D, Stereoselective Polymerization of Conjugated Dienes. in Encyclopedia of Polymer Science and Technology; Wiley: New York, 2013; pp 1–25.
- (4). For review on hydrofunctionalizations of 1,3-dienes, see: Adamson NJ, Malcolmson SJ, ACS Catal. 2020, 10, 1060–1076.
- (5). Löber O, Kawatsura M, Hartwig JF, J. Am. Chem. Soc. 2001, 123, 4366–4367. [PubMed: 11457216]
- (6). Yang X-H, Dong VM, J. Am. Chem. Soc. 2017, 139, 1774–1777. [PubMed: 28128936]
- (7). Adamson NJ, Hull E, Malcolmson SJ, J. Am. Chem. Soc. 2017, 139, 7180–7183. [PubMed: 28453290]
- (8). Tran G, Shao W, Mazet C, J. Am. Chem. Soc. 2019, 141, 14814–14822. [PubMed: 31436415]
- (9). For Mayr's Database of Reactivity Parameters, see: <https://www.cup.lmu.de/oc/mayr/reaktionsdatenbank/fe/>.

- (10). Haydl AM, Xu K, Breit B, *Angew. Chem. Int. Ed.* 2015, 54, 7149–7153; *Angew. Chem.* 2015, 127, 7255–7259; (b) Hilpert LJ, Sieger SV, Haydl AM, Breit B, *Angew. Chem. Int. Ed.* 2019, 58, 3378–3381; *Angew. Chem.* 2019, 131, 3416–3419.
- (11). Jiang W-S, Ji D-W, Zhang W-S, Zhang G, Min X-T, Hu Y-C, Jiang X-L, Chen Q-A, *Angew. Chem. Int. Ed.* 2021, 60, 8321–8328; *Angew. Chem.* 2021, 133, 8402–8409.
- (12). Yang X-H, Lu A, Dong VM, *J. Am. Chem. Soc.* 2017, 139, 14049–14052. [PubMed: 28953374]
- (13). (a) Lu G, Liu RY, Yang Y, Fang C, Lambrecht DS, Buchwald SL, Liu P, *J. Am. Chem. Soc.* 2017, 139, 16548–16555; [PubMed: 29064694] (b) Wagner JP, Schreiner PR, *Angew. Chem. Int. Ed.* 2015, 54, 12274–12296; *Angew. Chem.* 2015, 127, 12446–12471; (c) Ahlquist MSG, Norrby P-O, *Angew. Chem. Int. Ed.* 2011, 50, 11794–11797; *Angew. Chem.* 2011, 123, 11998–12001; (d) Johnson ER, Keinan S, Mori-Sánchez P, Contreras-García J, Cohen AJ, Yang W, *J. Am. Chem. Soc.* 2010, 132, 6498–6506. [PubMed: 20394428]
- (14). (a) Cruz FA, Dong VM, *J. Am. Chem. Soc.* 2017, 139, 1029–1032; [PubMed: 28074655] (b) Cruz FA, Zhu Y, Terceño QD, Shen Z, Dong VM, *J. Am. Chem. Soc.* 2017, 139, 10641–10644. [PubMed: 28742333]
- (15). Aguilar-Parrilla F, Cativiela C, de Villegas MDD, Elguero J, Foces-Foces C, Laureiro JIG, Cano FH, Limbach H-H, Smith JAS, Toiron C, *J. Chem. Soc. Perkin Trans. 2*, 1992, 2, 1737–1742.
- (16). For Rhodium-catalyzed hydroarylation of 1,3-dienes with indoles for C-allylation, see: Marcum JS, Roberts CC, Manan RS, Cervarich TN, Meek SJ, *J. Am. Chem. Soc.* 2017, 139, 15580–15583. [PubMed: 29058881]
- (17). Nitrogen labeling of pyrazole products is based on the product, i.e., the major product is the N^1 product. Triazole, indazole, and benzotriazole are labeled based on their naming conventions, i.e., the major products are the N^2 products.
- (18). To buffer the conditions as demonstrated by Malcomson,⁷ we added base (Et_3N) to the benzotriazole reaction, however, we saw no marked improvement, only decreased $N^2:N^1$ selectivity of 1:1.
- (19). (a) Furche F, Ahlrichs R, Wachsmann C, Weber E, Sobanski A, Vögtle F, Grimme S, *J. Am. Chem. Soc.* 2000, 122, 1717–1724; (b) Berova N, Di Bari L, Pescitelli G, *Chem. Soc. Rev.* 2007, 36, 914–931. [PubMed: 17534478]
- (20). In the cited mechanism, dissociation of one of the phosphine arms occurs, which is reasonable to consider. For more information, see: Zhang Q, Dong D, Zi W, *J. Am. Chem. Soc.* 2020, 142, 15860–15869. [PubMed: 32813509]
- (21). Benn R, Jolly PW, Joswig T, Mynott R, Schick K-P, *Naturforsch Z.* 1986, 41b, 680–691.
- (22). Wu Z, Zhang M, Shi Y, Huang G, *Org. Chem. Front.* 2020, 7, 1502–1511.
- (23). Bernar I, Fiser B, Blanco-Ania D, Gómez-Bengoá E, Rutjes FPJT, *Org. Lett.* 2017, 19, 4211–4214. [PubMed: 28786679]
- (24). Burés J, *Angew. Chem. Int. Ed.* 2016, 55, 16084–16087; *Angew. Chem.* 2016, 128, 16318–16321.
- (25). Zell D, Bursch M, Müller V, Grimme S, Ackermann L, *Angew. Chem. Int. Ed.* 2017, 56, 10378–10382; *Angew. Chem.* 2017, 129, 10514–10518.
- (26). (a) Sha S-C, Zhang J, Carroll PJ, Walsh PJ, *J. Am. Chem. Soc.* 2013, 135, 17602–17609; [PubMed: 24147620] (b) Trost BM, van Vranken DL, *Chem. Rev.* 1996, 96, 395–422. [PubMed: 11848758]
- (27). Nie S-Z, Davison RT, Dong VM, *J. Am. Chem. Soc.* 2018, 140, 16450–16454. [PubMed: 30451496]

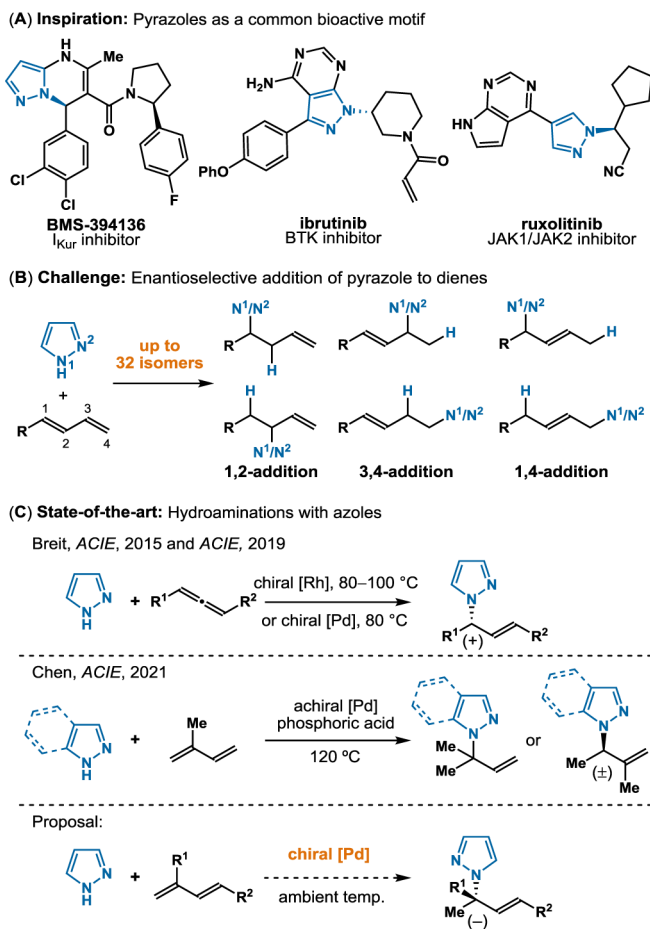


Figure 1. Inspiration for asymmetric hydroamination of 1,3-dienes with pyrazoles.

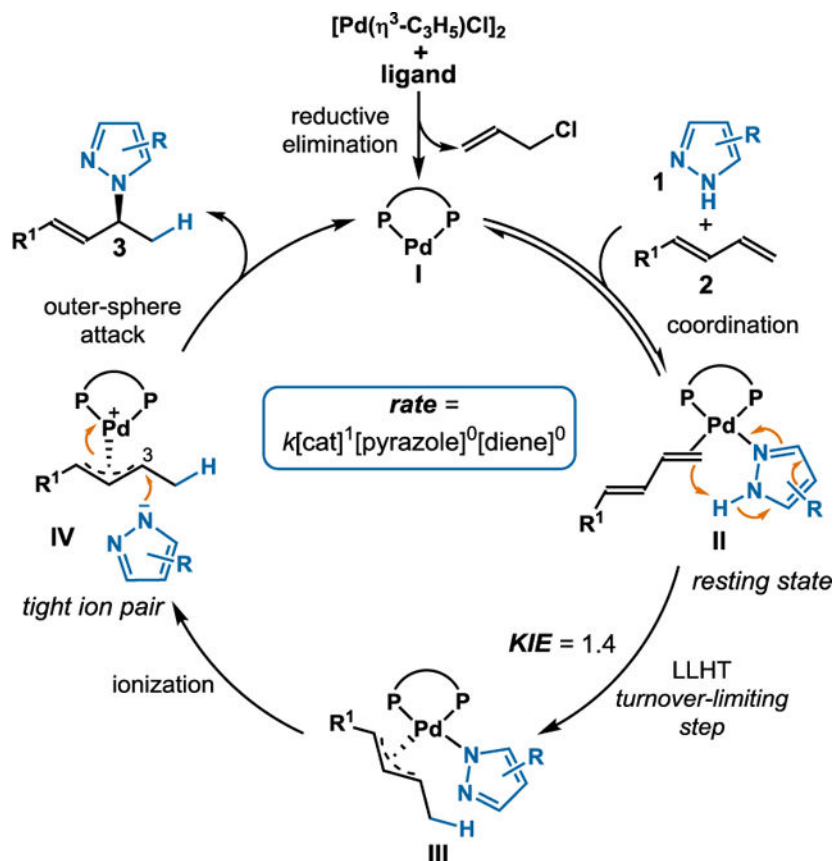


Figure 3.
Proposed mechanism.

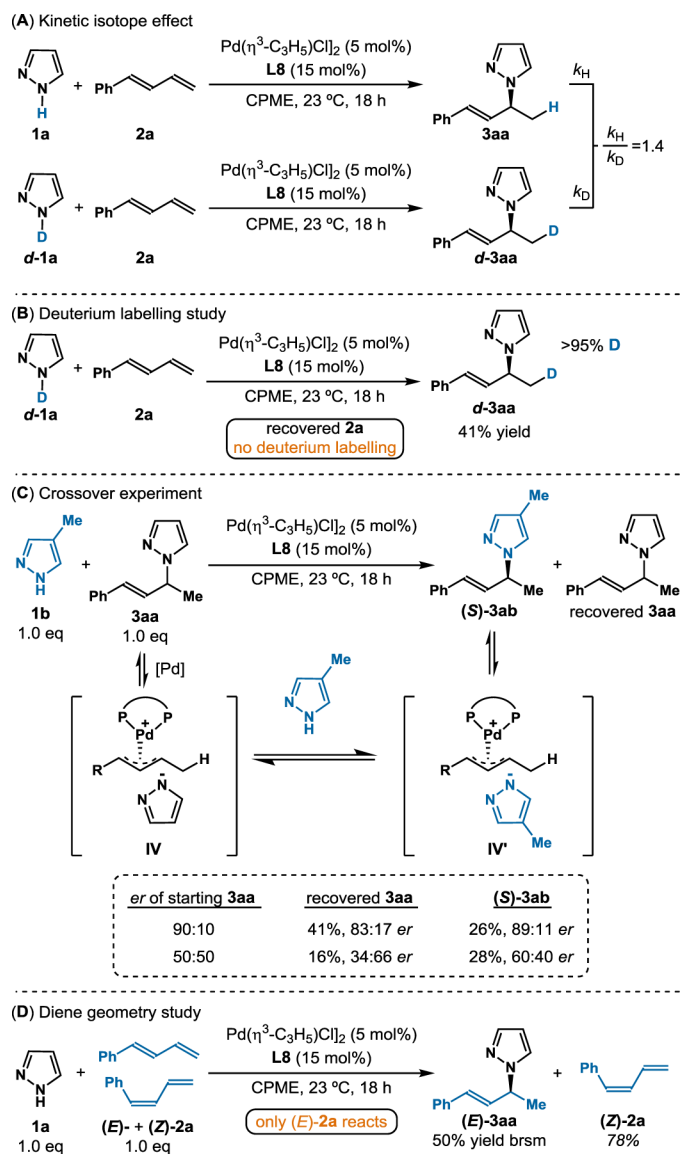
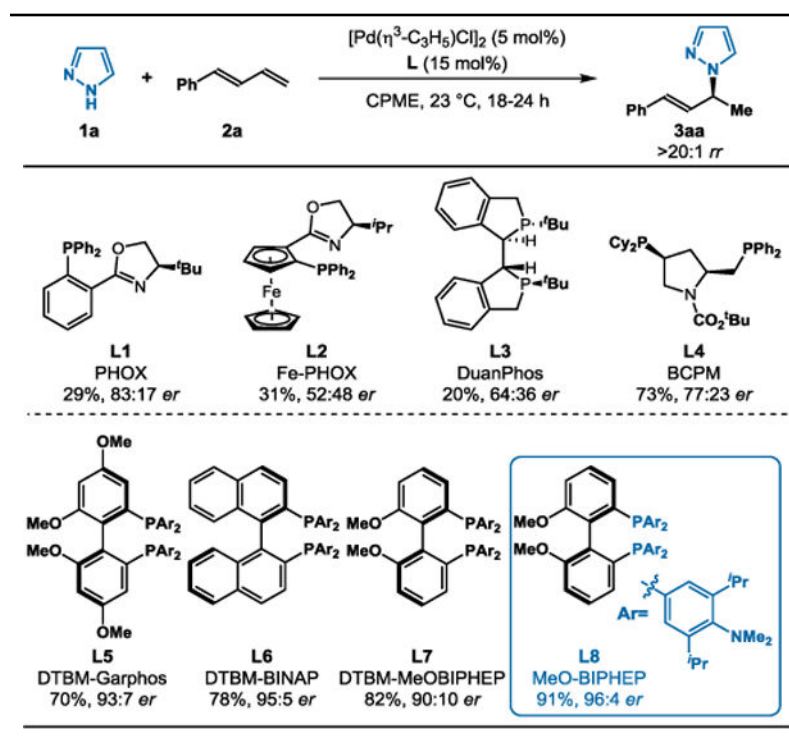


Figure 4.
Mechanistic studies.

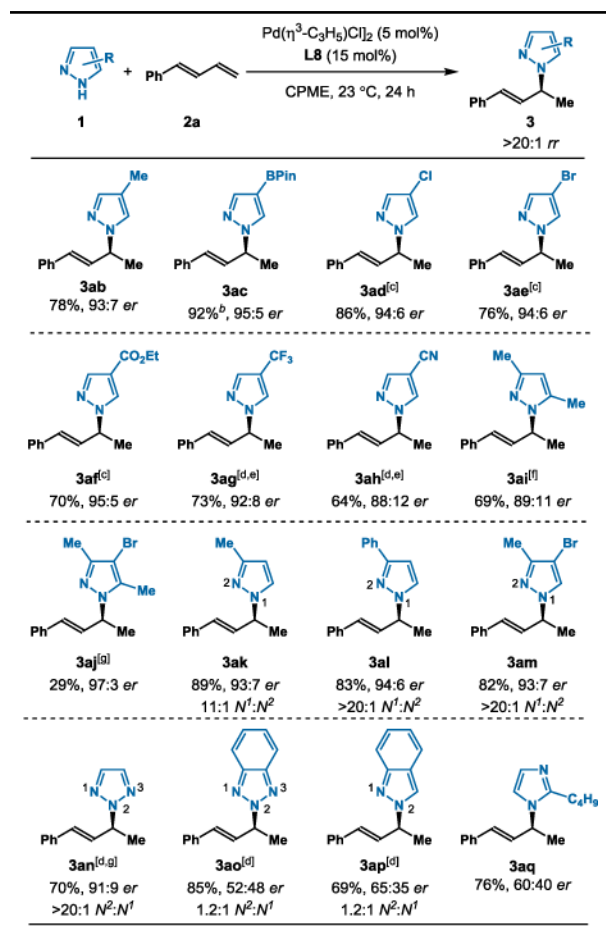
Table 1.

Ligand Effects on Asymmetric Pyrazole Hydroamination



Reaction conditions: **1a** (0.1 mmol), **2a** (0.5 mmol), $[\text{Pd}(\eta^3\text{-C}_3\text{H}_5\text{Cl})_2]$ (5 mol%), Ligand (15 mol%), CPME (0.4 mL), 23 °C, 18–24 h. Isolated yields. Regioselectivity determined by ^1H NMR analysis of the unpurified reaction mixture. Enantioselectivity determined by chiral SFC. DTBM = 3,5-di-*tert*-butyl-4-methoxyphenyl.

Table 2.

Hydroamination of 1,3-Diene (**2a**) with Various Azoles^[a]

^[a]Reaction conditions: **1** (0.2 mmol), **2a** (1.0 mmol), [Pd(η^3 -C₃H₅)Cl₂] (5 mol%), MeO-BIPHEP **L8** (15 mol%), CPME (0.8 mL), 23 °C, 24 h. Isolated yields. Regioselectivity determined by ¹H NMR analysis of the unpurified reaction mixture. Enantioselectivity determined by chiral SFC.

^[b]NMR yield.

^[c]48 h

^[d]60 °C

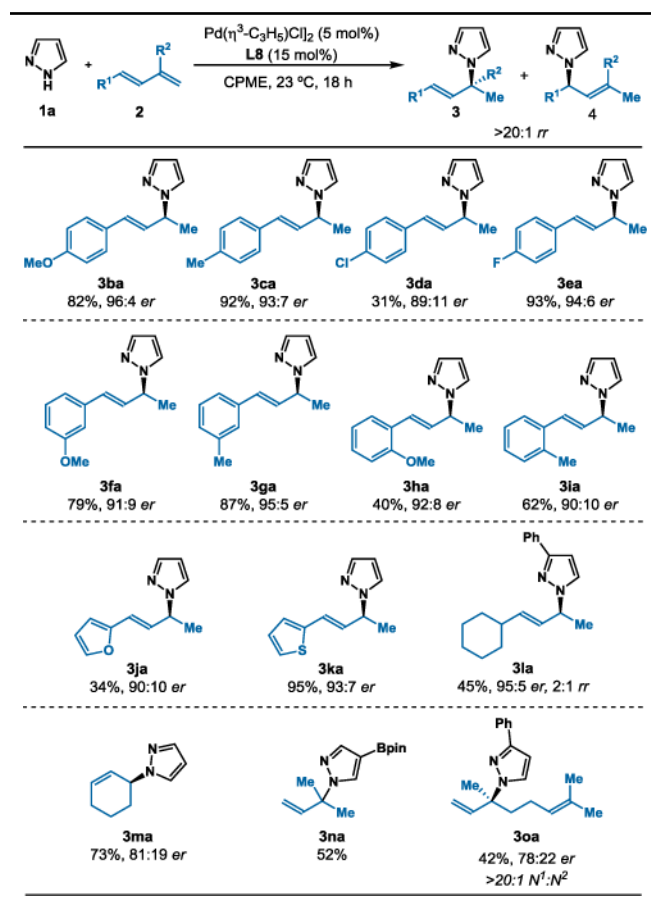
^[e]12 h

^[f]8 h

^[g]36 h.

Table 3.

Hydroamination of Various 1,3-Dienes with Pyrazole (1a)



Reaction conditions: **1a** (0.1 mmol), **2** (0.5 mmol), $[\text{Pd}(\eta^3\text{-C}_3\text{H}_5)\text{Cl}_2]$ (5 mol%), MeO-BIPHEP **L8** (15 mol%), CPME (0.4 mL), 23 °C, 18 h.

Isolated yields. Regioselectivity determined by ¹H NMR analysis of the unpurified reaction mixture. Enantioselectivity determined by chiral SFC.